Electric conduction mechanisms and metal-semiconductor transition in undoped amorphous ZnO thin films prepared by spray pyrolysis technique

F. HIJAZI[a,b], H. GHAMLOUCHE[a,*], N. CHOUEIB[a], R. SAYED HASSAN[a], B. LUCAS[b]
[a]*Lebanese University, Department of Physics, Faculty of Sciences I, Hadath, Beirut, Lebanon*
[b]*XLIM UMR 6172 – Université de Limoges/CNRS 123 Avenue Albert Thomas – 87060 Limoges Cedex, France*

In this work, the structural, electrical and optical properties of undoped ZnO amorphous thin films using Spray Pyrolysis deposition technique are presented. The structural measurements (XRD) show that for a film of thickness 20 nm, the material is in the amorphous phase. Therefore, this work is focused on the film of this thickness (20 nm). From the optical measurements, a transmission of 85 % as well as an energy-gap of 3.15 eV have been obtained. The electric conductivity and the Seebeck coefficient show a semiconductor-metal transition at around 305 K. Up to our knowledge, this transition is observed for the first time in amorphous ZnO thin films. It might be due to the oxygen adsorption above room temperature. In addition, three regimes are identified for the conduction mechanisms from the variation of both the electric conductivity and the Seebeck coefficient as a function of temperature. The standard transport model is used in order to interpret the behavior of the conductivity and the Seebeck coefficient. At low temperatures ($T < 255$ K), the conduction mechanism is dominated by the hopping between localized states. At temperatures $255 < T < 275$ K, a brisk change in the conductivity and the Seebeck coefficient curves is observed; it might correspond to a transition zone of certain localized states close to the conduction band. At the end, for temperatures $275 < T < 305$ K, the conduction mechanism is dominated by the non-localized states.

(Received September 15, 2016; accepted August 9, 2017)

Keywords: ZnO, Amorphous semiconductor, Thin film, Spray Pyrolysis, Conduction mechanisms, Amorphous-metal transition

1. Introduction

Since zinc oxide ZnO is a semiconductor material with a wide band gap of 3.27 eV and a large exciton binding energy of 60 meV at room temperature, ZnO-based thin films have been used for several applications such as transparent conducting oxide TCO, ultraviolet light emitters, solar cell windows, and bulk acoustic wave devices [1-4].

On the other hand, the reduction of thin films to nanometer dimensions for new technologies requires precise control of film thickness, conformity, and morphology. ZnO is known to be a transparent material. It is normally a non-degenerate semiconductor, but it can exhibit a relatively high conductivity [5] due to the many defects such as stoichiometric excess of zinc and vacancies introduced in the sample during film deposition. Generally, this oxide is also considered to be an n-type material due to oxygen deficiencies and interstitial Zn, which act as donors in the ZnO lattice [6].

Spray pyrolysis technique has been widely used in the deposition of doped and undoped ZnO [7-13]. This technique has the advantages of low cost, easy-to-use, high growth rates, safety and can be implemented for large area depositions. Using this technique it is rather easy to vary the doping concentrations and hence to tailor the properties of the ZnO films [7].

Transport properties of these oxides depend on the deposition technique, film quality as well as film thickness. In particular, the electric conduction mechanisms depend on the structural properties of the thin films. Many studies on polycrystalline doped and undoped ZnO thin films prepared by different techniques have been reported [14-16]. In these studies, a metal-semiconductor transition was observed and investigated. In particular, N. Kavasoglu et al. [16] are the only group (up to our knowledge) who has reported work about such transition on polycrystalline undoped ZnO thin films using ultrasonic spray pyrolysis technique.

In the present work, electric conduction mechanisms and metal-semiconductor transition phenomenon in amorphous undoped ZnO thin films prepared by spray pyrolysis technique will be presented and investigated.

2. Experimental

The well-known spray pyrolysis technique is a process in which a thin film is deposited by spraying a solution on a heated surface. The chemical precursors are selected such that the products other than the desired compound are volatile at the temperature of deposition. The process is particularly useful for the deposition of oxides and has long been a production method for

applying transparent electrodes. Undoped ZnO thin films have been deposited on a glass substrate. The precursor solution has been prepared starting with a mixture of 2.4 g of $Zn(CH_3COO)_2$ powder in different methanol volumes (with and without deionized water). The optimal parameters for the deposition have been chosen after many attempts in order to obtain an optimal electric conductivity. These parameters are: the concentration of zinc is 80 mg/ml, the solvent volume is 25 ml of methanol and 5 ml of deionized water, the deposition temperature is 500^oC.

The structural characterization of the films, for different thicknesses, was carried out by X-Ray diffraction technique using an X-Ray diffractometer (Bruker D5000) with CuK_α radiation ($\lambda = 1.5418$Å).

The optical transmission of the films was determined using a double beam UV-VIS-NIR spectrophotometer (SAFAS 200 DES) with 170-1010 nm wavelength range and 1 nm resolution.

The electric conductivity and the thermopower measurements have been performed simultaneously using a home-made four probes technique, detailed elsewhere [17].

3. Results and discussions

The XRD was used to analyze the growth orientation and to determine the main crystalline phases of undoped ZnO thin films. Fig. 1 shows the XRD spectra for different films thicknesses: 20 nm, 60 nm, 80 nm, 120 nm and 160 nm. For the film of 20nm, it is obvious that the film is in the amorphous phase since there are no structures in the spectrum.

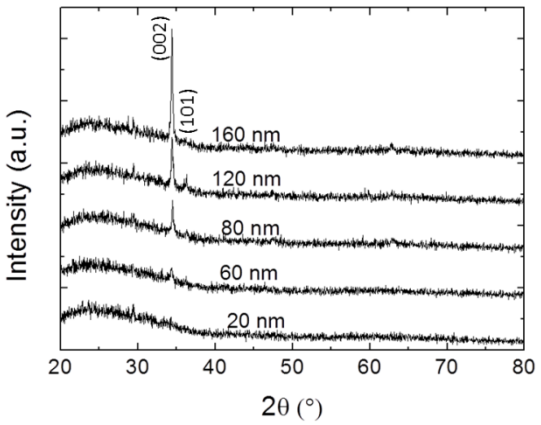

Fig. 1. XRD pattern of ZnO for different thicknesses of the thin films (20nm, 60nm, 80nm, 120nm and 160nm). For the film of 20 nm, it is obvious that the film is in the amorphous phase

This figure shows that above a thickness of 80 nm the ZnO films start to be preferably oriented along a direction perpendicular to the crystallographic planes (002), with a diffraction peak at $2\theta = 34.56^o$; this peak is more pronounced as the film thickness increases. For the undoped ZnO (002) and (101) peaks are much pronounced than all other peaks. This implies that this film exhibits a random orientation due to the fact that crystallites grew randomly on glass substrate. On the other hand, for 20 nm thickness the film seems to be in the amorphous phase since no crystallographic peaks were observed. The film with 20 nm thickness will be investigated in this paper as it is in the amorphous phase.

Fig. 2 shows the optical transmittance spectrum of amorphous undoped ZnO (20nm thickness) measured at room temperature. The transmittance spectrum revealed that the film has a high average transmittance above 85%.

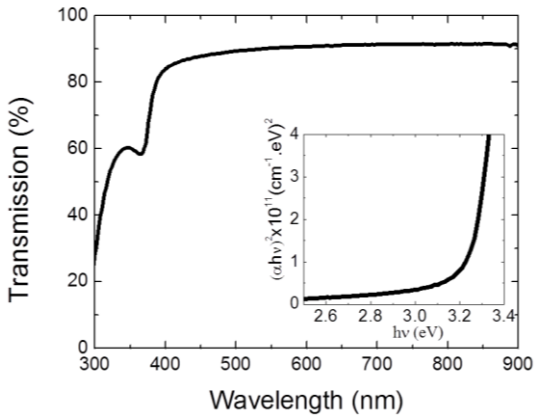

Fig. 2. Transmission spectrum as a function of the wavelength. The inset shows the variation of $(\alpha hv)^2$ as a function of the incident photon energy (hv)

From Fig. 2, the bandgap of the film can be calculated from fundamental absorption spectrum of the film. The absorption coefficient α is calculated using the transmission spectrum and the equation $\alpha = (ln\frac{1}{T})/d$, where T is the transmittance and d is the thickness of the film. The absorption coefficient, as shown in the inset of Fig. 2, has been expressed by M. Caglar et al. [18]

$$(\alpha hv)^2 = A(hv - E_g) \quad (1)$$

Where A is a function of the refractive index and hole (electron) effective mass, E_g is the energy gap, h is the Plank's constant and v is the frequency of the incident radiation. From this expression, one can deduce the energy gap that is 3.15eV. Similar results have been obtained for ZnO films deposited by sol-gel technique [19-20].

Fig. 3 shows the variation of the electric conductivity and the Seebeck coefficient versus the inverse temperature. At low temperatures T < 255 K (Region I), the conductivity increases linearly with temperature. At the same time, the Seebeck coefficient decreases linearly while remaining negative.

For temperatures between 255 K and 275 K (Region II), the conductivity curve shows a brisk change with temperature and correspondingly a change in the slope in the Seebeck coefficient. At intermediate temperatures between 275 K and 305 K (Region III), a thermally activated regime has been observed. For 305 < T < 360 K

(Region IV), a sudden drop of the conductivity has been observed.

For T > 360 K, above region IV, the conductivity changes its behavior while continuing decrease.

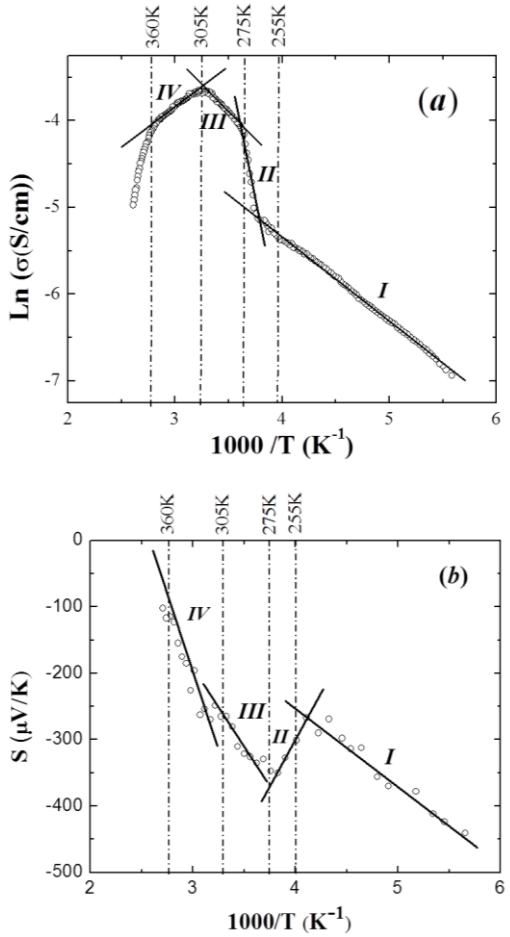

Fig. 3. Variation of the Ln of the electric conductivity (a) and the Seebeck coefficient (b) as a function of inverse temperature. The Thickness of the samples is 20 nm in both measurements

Now in order to explain the behavior of the conductivity and the Seebeck coefficient shown in Fig. 3, one should choose an appropriate model that is able to describe the conduction mechanisms in the amorphous semiconductors. In contrast to their crystalline counterparts, amorphous semiconductors feature pronounce disorder instead of a periodic potential. Therefore, the situation in amorphous semiconductors involves new concepts such as "band tails" and "mobility edges". Different models have been proposed in order to describe the conduction mechanisms in amorphous semiconductors [21]. The standard transport model is considered the basic one and it is based on the following assumptions: 1) The one-particle approximation holds, i.e. electron-electron interaction effects can be neglected. 2) Charge transport processes at different energies can be treated separately, i.e. conduction does not interconnect states of different energies. If energy exchange between the electronic system and the lattice is allowed (e.g. phonon-assisted hopping), this assumption becomes questionable. 3) The solid is homogeneous, i.e. the potential experienced by the electrons features no long-ranged but exclusively local fluctuations. According to this model, two different conduction mechanisms can be considered. At low temperatures, the conduction is due to hopping between localized states (hopping transport). At higher temperatures, the conduction is dominated by the non-localized states (extended state transport). Taking the above mentioned two different mechanisms, the electric conductivity and the Seebeck coefficient are given by:

$$\sigma_{ext\,(hop)} = \sigma_0 \exp\left(-\frac{E_\sigma}{k_B T}\right) \tag{2}$$

$$S_{ext(hop)} = \pm \frac{k_B}{e}\left(\frac{E_S}{k_B T} + A\right) \tag{3}$$

where, the activation energies equal the energetic distance between the Fermi level and the mobility edge, the pre-exponential factor of the conductivity corresponds to the minimum metallic conductivity, and A is the heat-of-transport constant. The sign of the thermopower depends on whether the mobility edge above (electrons, "-") or below (holes, "+") the Fermi level is considered [22-24]. In our case, the negative (-) sign has been chosen in Eq. (3) since the ZnO film is an n-type semiconductor. The subscript (*ext*) is for extending state and (*hop*) for hopping state.

As mentioned above, this model has been used to fit our experimental data. For temperatures less than 255K (Region I), the conduction mechanism is associated with the carrier displacement within the localized states. From Fig. 2 (a) and (b) one can determine the activation energies for the electric conductivity and Seebeck coefficient based on Eqs. (2) and (3). The results are filled in Table 1.

For temperatures between 255K and 275K (Region II), the sharp transition might correspond to a transition zone of certain localized states close to the conduction band. This behavior has not been observed before, up to our knowledge, but it could be related to the preparation technique. This later has a great influence on the quality of the films and the types of defects that are produced.

In region III (275 < T < 305), a change in the slope is observed as shown in Table 1. This behavior might be related to conduction of non-localized states.

Table 1. This table summarizes the fitting parameters of Eqs. (2) and (3)

	Slopes		**Intercepts**	
Regime	**E_σ (meV)**	**E_S (meV)**	**σ_0 (S/cm)**	**A**
Low temperature (185 – 255 K)	86	120	0.3	2.7
High temperature (275 - 305 K)	115	161	2.2	3.6

In region IV (305 < T < 360 K), the sudden drop in the conductivity might be due to certain adsorption phenomena that depend on the thickness of the film, structure (amorphous or polycrystalline), grains' dimensions, density, defects, etc. This behavior has been observed in crystalline ZnO thin films [16], but up to our knowledge, this is the first time that this behavior is observed in amorphous ZnO thin films. It has been attributed to a Metal-Semiconductor transition.

Above region IV (T > 360 K), a change in the slope has been observed. This could be due to the fact that we are approaching the amorphous-crystalline transition temperature. It has been observed that the conductivity in ZnO decreases at the transition from amorphous to crystalline phase [25] unlike other materials such as phase change materials that are used in optical and electrical data storage [26].

4. Conclusion

In this work, the structural, electrical and optical properties of undoped ZnO amorphous thin films using Spray Pyrolysis deposition technique have been presented. From the structural measurements (XRD), one can observe that for a film thickness of 20 nm the material is in the amorphous phase. Therefore, the remaining part of this work has been done on the film of thickness of 20 nm (in the amorphous phase). From the optical measurements, the transmission (above 85 %) and the energy gap (3.15 eV) have been determined. The electric conductivity and the Seebeck effect show a semiconductor-metal transition at around 305 K that might be related to the oxygen adsorption above room temperature. In addition, three regimes have been identified for the conduction mechanisms from the variation of both the electric conductivity and the Seebeck coefficient as a function of temperature. The standard transport model has been used in order to interpret the behaviour of the conductivity and the Seebeck coefficient. At the end, the doping process and implementation of ZnO in certain applications especially solar cells are under investigations.

References

[1] C. Jagadish, S. Pearton, Zinc Oxide Bulk, Thin Films and Nanostructures, Edited by Chennupati Jagadish and Stephan J. Pearton (Oxford UK: Elsevier) (2006).

[2] J. N. Duenow, T. A. Gessert, D. M. Wood, T. M. Barnes, M. Young, B. To, T. J. Coutts, Journal of Vacuum Science & Technology A, **25**(4), 955 (2007).

[3] T. Minami, H. Nanto, S. Takata, Japanese Journal of Applied Physics **23**(5), L280 (1984).

[4] F. K. Shan, G. X. Liu, W. J. Lee, B. C. Shin, J. Appl. Phys. **101**(5), 053106 (2007).

[5] B. Lucas, A. El Amrani, A. Moliton, M. Dilhan, Superlattices Microstruct. **42**(1-6), 357 (2007).

[6] D. H. Zhang, Z. Y. Xue, Q. P. Wang, J. Phys. D: Appl. Phys. **35**(21), 2837 (2002).

[7] S. S. Shinde, P. S. Shinde, C. H. Bhosale, K. Y. Rajpure, Journal of Physics D: Applied Physics **41**(10), 105109 (2008).

[8] S. S. Shinde, P. S. Shinde, S. M. Pawar, A. V. Moholkar, C. H. Bhosale, K. Y. Rajpure, Solid State Sciences **10**(9), 1209 (2008).

[9] S. S. Shinde, C. H. Bhosale, K. Y. Rajpure, Journal of Photochemistry and Photobiology B: Biology **113**, 70 (2012).

[10] S. S. Shinde, Prakash S. Patil, R. S. Gaikwad, R. S. Mane, B. N. Pawar, K. Y. Rajpure, Journal of Alloys and Compounds **503**(2), 416 (2010).

[11] S. S. Shinde, K. Y. Rajpure, Materials Research Bulletin **46**(10), 1734 (2011).

[12] S. S. Shinde, P. S. Shinde, Y. W. Oh, D. Haranath, C. H. Bhosale, K. Y. Rajpure, Applied Surface Science **258**(24), 9969 (2012).

[13] S. S. Shinde, K. Y. Rajpure, Journal of Alloys and Compounds **522**, 118 (2012).

[14] P. Banerjee, W. J. Lee, K. R. Bae, S. B. Lee, G. W. Rubloff, J. Appl. Phys. **108**, 043504 (2010).

[15] E. L. Papadopoulou, M. Varda, K. Kouroupis-Agalou, M. Androulidaki, E. Chikoidze, P. Galtier, G. Huyberechts, E. Aperathitis, Thin Solid Films **516**(22), 8141 (2008).

[16] N. Kavasoglu, A. S. Kavasoglu, J. Phys. B **403**(17), 2807 (2008).

[17] A. Moliton, B. Ratier, C. Moreau, G. Froyer, J. Phys. III **1**, 809 (1991).

[18] M. Caglar, S. Ilican, Y. Caglar, Thin Solid Film **517**(17), 5023 (2009).

[19] A. Jain, P. Sagar, R. M. Mehra, Materials Science-Poland **25**(1), 233 (2007).

[20] S. Mridha, D. Basak, Materials Research Bulletin **42**(5), 875 (2007).

[21] H. Overhof, P. Thomas, "Hydrogenated Amorphous Semiconductors" (Springer-Verlag, Berlin), 14th edn (1989).

[22] S. R. Elliot, "Physics of amorphous materials" (Longman, London) (1989).

[23] H. Fritzsche, "A General expression for the thermoelectric Power" Sol. Stat. Comm. **9**, 1813 (1971).

[24] R. A. Street "Hydrogenated amorphous silicon", Cambridge solid state science series (Cambridge University Press, Cambridge) (1991).

[25] A. El Amrani, F. Hijazi, B. Lucas, J. Bouclé, M. Aldissi, Thin Solid Films **517**(17), 5023 (2009).

[26] S. T. Mahmoud, N. Qamhieh, A. I. Ayesh, H. Ghamlouche, M. El-Shaer, J. Optoelectron. Adv. M. **13**(11-12), 1498 (2011).

*Corresponding author: hassan.ghamlouche@ul.edu.lb